Convertible transmission-reflection time-domain terahertz spectrometer

Max Khazan,[a] Reinhold Meissner, and Ingrid Wilke
Institut für Angewandte Physik, Universität Hamburg, Jungiusstrasse 11, D-20355 Hamburg, Germany

(Received 19 February 2001; accepted for publication 11 May 2001)

The creation of reliable instrumentation for performing complex reflectance and transmittance measurements of dielectrics, metals, and superconductors in the frequency range from 60 GHz to 1.5 THz is reported. The system allows continuous variation of the THz radiation incidence angle from 25° to 80° without major realignment of the optics and provides the signal-to-noise ratio of 1000:1. © *2001 American Institute of Physics.* [DOI: 10.1063/1.1384433]

I. INTRODUCTION

In the last decade, time-domain terahertz spectroscopy (TDTS)[1] has become a powerful means to study properties of various materials from dielectrics to semiconductors[2] and superconductors.[3,4] More recently, TDTS has been successfully applied to precise gas sensing.[5,6] TDTS operates with subpicosecond pulses of electromagnetic radiation which in the frequency domain implies coverage of a very broad range spanning from tens of gigahertz to few terahertz. Thus, TDTS bridges a large frequency gap between microwave and conventional infrared spectroscopy. Moreover, being a phase-sensitive method, it allows the extraction of the *complex* refractive index of a material from *either* transmission or reflection data without the use of Kramers–Kronig analysis. In most of materials science applications, the transmission configuration of TDTS (TTDTS) is employed. This method is well developed and reliable but is obviously applicable only to transparent samples. Therefore, highly conductive materials can be studied with TTDTS only in the form of thin films, and for measurements on bulk samples the TDTS in reflection geometry (RTDTS) becomes the only choice. Various perspective THz imaging applications[7] especially THz tomography[8] are also based on the measurement of the complex reflectivity. To date, there have been only few works published reporting realization of the RTDTS.[9,10] Such systems appear difficult to adjust since a change of the incidence angle requires a complete realignment of the whole spectrometer. Thus, the creation of a time-domain THz spectrometer that allows easy change of the incidence angle along with measurements in transmission configuration significantly extends the area of the TDTS applications.

II. EXPERIMENTAL SETUP

A. Transmission configuration

In the transmission configuration, the convertible time-domain THz spectrometer is identical to the experimental arrangements widely described in the literature.[11,12] Our setup (Fig. 1) is powered by a Spectra-Physics' Tsunami Ti: sapphire laser (pulse length 50 fs, central wavelength 780 nm, average power 650 mW) and operates according to the pump–probe scheme whose principle can be briefly described as follows. The initial laser beam is split in two parts. One of them, the pump beam, hits an emitter which in the response to the optical pulse releases a subpicosecond pulse of THz radiation. The probe beam gates the detector whose response is proportional to the amplitude and the sign of the electric field of the THz pulse. By varying the delay between pump and probe pulses the whole time profile of the THz pulse is traced. Then the complex transmittance of a sample is given as the ratio of the Fourier transforms of a pulse transmitted through the sample and a reference, e.g., freely propagating pulse.

As an emitter of THz radiation we use a large-aperture low-temperature-grown GaAs[13] photoconductor dc biased at 1800 V. The emitted radiation is guided from the emitter through a sample onto a detector by a classical sequence of four off-axis parabolic mirrors from Janos Technology, Inc. The mirrors' diameter is 50.8 mm and the effective reflected focal lengths are 50.8, 152.4, 152.4, and 50.8 mm for the parabolic mirrors PM I, PM II, PM III, and PM IV, respectively. The detector is a silicon-on-sapphire antenna endowed with a 6 mm hemispherical silicon lens for additional focusing of the incident radiation. The THz beam is polarized horizontally, i.e., in the plane of the figure. For polarization sensitive measurements, an additional tungsten-wire grid polarizer (wire diameter 10 μm, period 33 μm) is set between PM I and PM II (not shown). Such an arrangement permits measurements of the complex transmittance in the frequency range from 60 GHz to 1.5 THz with a signal-to-noise ration of at least 1000:1.

B. Reflection configuration

In order to make the spectrometer transmission-reflection convertible and to enable a smooth change of the incidence angle, all optical elements are installed on an aluminum adjustable frame with five pivotal points (Fig. 2). The positions of points 1 and 5 are fixed and points 2, 3, and 4 are movable. A sample holder is placed at point 3 so that the sample always stays in the common focus of the paraboloids II and III. The threaded control rod allows smooth movement of the point so that the THz radiation incidence angle is

[a]Author to whom correspondence should be addressed; electronic mail: khazan@physnet.uni-hamburg.de

 © 2001 American Institute of Physics

Downloaded 16 Jan 2002 to 128.113.8.139. Redistribution subject to AIP license or copyright, see http://ojps.aip.org/rsio/rsicr.jsp

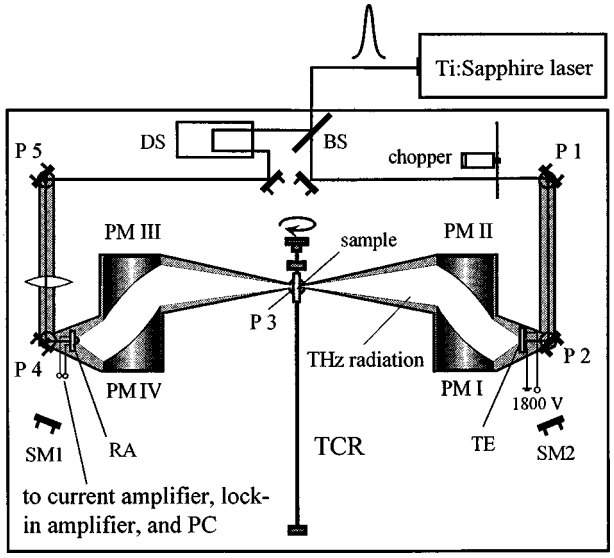

FIG. 1. The convertible time-domain THz spectrometer in transmission configuration: (BS) beam splitter, (TE) THz emitter, (RA) receiver antenna, (P1–P5) pivotal points, (PM I–PM IV) parabolic mirrors, (SM1) and (SM2) support optical mirrors, (TCR) threaded control rod, and (DS) delay stage.

continuously changed from 25° to 80°. The angle variation range is limited from below by the focal lengths of the parabolic mirrors II and III and by the dimensions of their holders. By use of paraboloids with longer focal lengths smaller angles of incidence can be achieved. At small incidence angles, when the optical beams strike the mirrors positioned in P2 and P4 under large angles, it is necessary to employ additional support mirrors SM1 and SM2 to guide the beams.

The use of the adjustable frame guarantees that the optical paths of the pump and probe beams remain unchanged. In order to change the angle of incidence, it is sufficient to readjust only the mirrors at the pivotal points. Moreover, once fixed in the transmission configuration, the four-paraboloid sequence requires no further tedious adjustments.

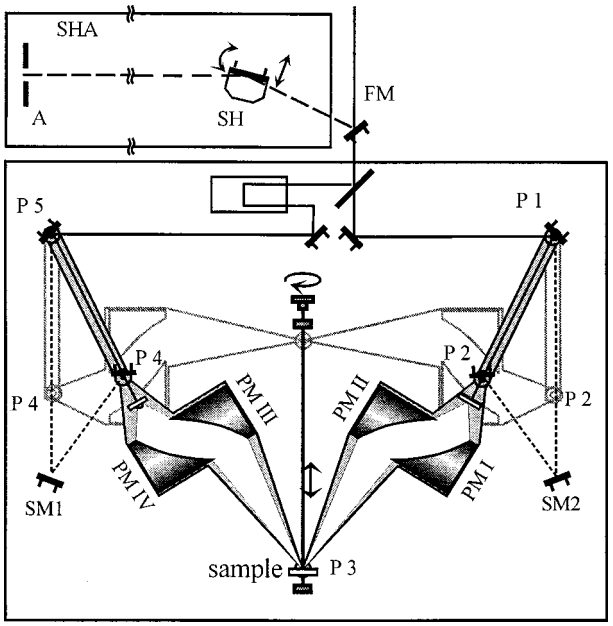

FIG. 2. The reflection configuration: (FM) flipper mirror, (SHA) sample holder adjuster, and (A) aperture.

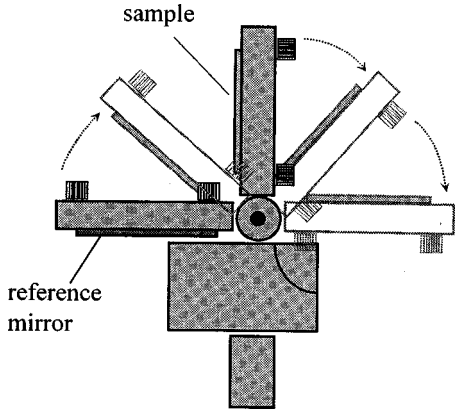

FIG. 3. The sample holder (side view).

As a sample holder, we use a modified New Focus flipper mirror mount (Fig. 3). The modification consists of two (instead of one) adjustable mirror holder frames being mounted on the flipper perpendicular to each other. A sample is attached to one frame and a reference silver mirror is held by another one so that the change between the sample and the mirror is done by flipping the mount.

The total time required for the change of the incidence angle, adjustment of pump and probe beams, and the measurement itself does not exceed 15 min. The precise control of sample position is a challenging experimental task in time-domain reflection spectroscopy.[14] Similarly to the case of measurement of the complex transmissivity, to obtain the frequency dependence of the complex reflectivity, it is necessary to perform two measurements: of the pulse reflected from a sample and the one reflected from a reference surface. Naturally, the sample and the reference mirror have to be consequently placed in the same point with the maximum precision possible, otherwise the phase information would be significantly distorted. Before the start of the reflectivity measurements, the sample and the reference mirror positions are adjusted in a sample holder adjuster (Fig. 2). The optical laser beam is picked up before the spectrometer and sent to the sample (or the reference mirror). Steering the reflected beam to make it pass through a narrow aperture we ensure that the sample's surface is set in the same position as the reference mirror with 100 μm precision. Then the holder is installed back to the pivotal point P3. However, in reality the mechanical adjustment is often not sufficient for phase-sensitive measurements. The ways to further improve the phase sensitivity are discussed in Sec. III B.

III. SAMPLE MEASUREMENTS AND DISCUSSION

A. Measurements of relative complex reflectivity

The effectiveness of the described technique has been tested by measuring the complex transmissivity and reflectivity of a 0.3-mm-thick high-resistivity silicon wafer ($\rho_0 = 10\,\mathrm{k}\Omega$ cm). In Fig. 4 the time profile of THz pulses for the cases of free-space propagation, transmission through the wafer, and surface reflection are shown. From transmission

Downloaded 16 Jan 2002 to 128.113.8.139. Redistribution subject to AIP license or copyright, see http://ojps.aip.org/rsio/rsicr.jsp

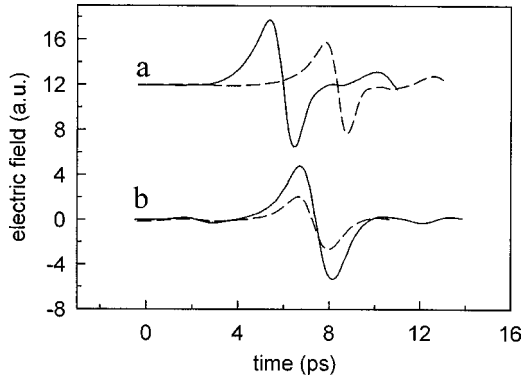

FIG. 4. Time-domain data: (a) reference, freely propagating pulse (solid line) and pulse transmitted through a silicon wafer (dashed line). (b) Reference, pulse reflected by a silver mirror (solid line) and pulse reflected from silicon wafer surface at 45° incidence (dashed line).

data the complex refractive index $n^*(\omega)=n(\omega)+ik(\omega)$ is calculated by numerically solving the Fresnel transmission equation

$$T^*(\omega)=\frac{4n^*\exp\left[-i\frac{\omega}{c}n^*d\right]}{(n^*+1)^2\left(1-\left(\frac{n^*-1}{n^*+1}\right)^2\exp\left[-2i\frac{\omega}{c}n^*d\right]\right)}, \tag{1}$$

where d is the thickness of the sample. The complex refractive index spectrum obtained this way is shown in Fig. 5. It is seen that the agreement with previously reported data[15] is excellent.

Then these values of n^* have been used for the calculation of the complex reflectivity through the Fresnel formula[16]

$$R_P^*(\Theta,n^*(\omega))=-\frac{n^{*2}(\omega)\cos\Theta-\sqrt{n^{*2}(\omega)-\sin^2\Theta}}{n^{*2}(\omega)\cos\Theta+\sqrt{n^{*2}(\omega)-\sin^2\Theta}}, \tag{2}$$

$$R_S^*(\Theta,n^*(\omega))=-\frac{\cos\Theta-\sqrt{n^{*2}(\omega)-\sin^2\Theta}}{\cos\Theta+\sqrt{n^{*2}(\omega)-\sin^2\Theta}}, \tag{3}$$

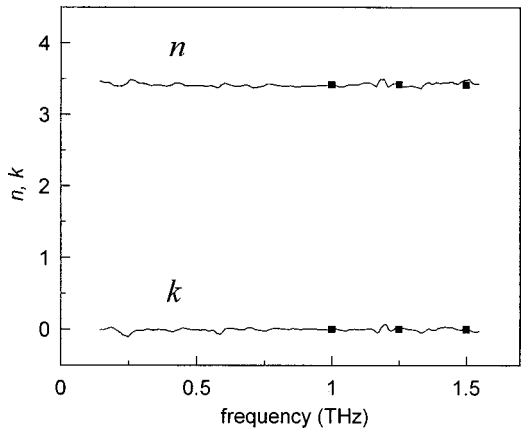

FIG. 5. Frequency dependence of the complex refractive index of high-resistivity silicon calculated from the measured complex transmissivity (solid line) and the data from Ref. 15 (points).

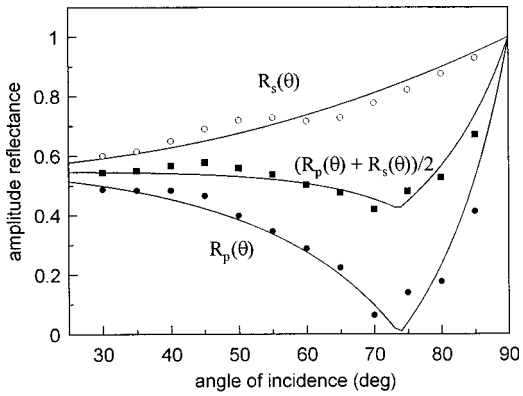

FIG. 6. Amplitude reflectivities of high-resistivity silicon for *s* and *p* polarizations at 0.4 THz. Solid lines are the ideal Fresnel reflectivities.

where Θ is the incidence angle of the THz radiation, and *s* and *p* polarizations imply that the THz beam is polarized perpendicular and parallel to the incidence plane.

In order to perform measurements of the reflectivity of *s*-polarized THz radiation, both the emitter and the detector antenna are turned for 90°.

Figure 6 shows measured amplitude reflectivities compared to the predictions of Eqs. (2) and (3). The measurements agree very well with the calculations. Some slight deviations of the measured data from the ideal Fresnel reflectivities are attributed to THz radiation being not perfectly *p* or *s* polarized so that some small fraction of unwanted polarization is always present. This effect manifests itself in a small minimum in $R_S(\Theta)$ and nonzero values of $R_P(\Theta)$ in the vicinity of the Brewster angle ($\Theta_B=73.7°$).

As has been mentioned in the Sec. II B, the measured phase of the complex reflectivity often needs an additional correction. Uncertainty in the position of a sample with respect to a reference mirror results in the reflected pulse acquiring an additional phase shift φ_0. This leads to errors in the determined refractive index which are particularly large in the case of weakly absorbing materials like silicon (see Fig. 7). The approaches to overcoming the problem are described in the following section.

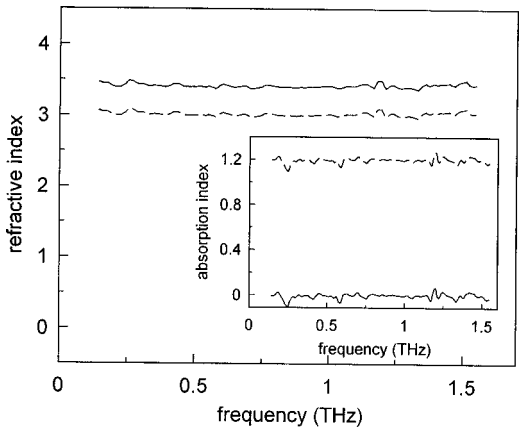

FIG. 7. Refractive index of high-resistivity silicon calculated from the complex reflectivity for *s* polarization (45° incidence): as measured (dashed line) and after the correction through Eq. (4) (solid line). The corresponding uncertainty in time domain is 48 fs.

Downloaded 16 Jan 2002 to 128.113.8.139. Redistribution subject to AIP license or copyright, see http://ojps.aip.org/rsio/rsicr.jsp

B. How to deal with phase uncertainty

1. Numerical correction of phase

Having measured the complex reflectivity for *either s* or *p* polarization, we can get rid of φ_0 with the help of a simple mathematical procedure. We introduce into Eqs. (2) and (3) a value of n_0^* calculated through Eq. (1) at some certain frequency ω_1 from measured transmissivity to obtain the corresponding complex reflectivity $R_0^*(\omega_1)$. Comparing it to the measured value of $R^*(\omega_1)$, we calculate φ_0 through Eq. (4):

$$e^{i\varphi_0} = \frac{R^*(\omega_1)}{R_0^*(\omega_1)} \tag{4}$$

and then subtract it from the phase of $R^*(\omega)$ at all frequencies. This method is simple and direct but its drawback is that the usage of Fresnel formulas [Eqs. (2) or (3)] is valid only when the reference surface can be treated as an ideal reflector compared to the sample.

2. Extraction of the refractive index from amplitude reflectivities

When the reflectivity is measured for *both s* and *p* polarization, the system of equations (2) and (3) is then solved in terms of *amplitude* reflectivities $|R_S^*(\omega)|$ and $|R_P^*(\omega)|$ to extract $n^*(\omega) = n(\omega) + ik(\omega)$. Now it is not necessary to calculate φ_0 but the supposition of the ideal reflectance of the reference surface should still be made.

3. Reference-free measurements

In principle, the polarization sensitivity of the THz emitter and the detector antenna allows the reference-free extraction of the complex refractive index of a sample's material. At some certain incidence angle Θ, instead of measurement of $R_S^*(\omega)$ and $R_P^*(\omega)$ which actually implies the scan of four time profiles (pulses reflected from the sample and the reference surface for either polarization), one obtains a complex function $\rho_{PS}^*(\omega)$ as a ratio of Fourier transforms of time profiles of the pulses reflected from the sample at *s* and *p* polarizations

$$\rho_{PS}^*(\omega) = \frac{E_P^*(\omega)}{E_S^*(\omega)} \tag{5}$$

or

$$\rho_{PS}^*(\omega) = \frac{R_P^*(\omega)}{R_S^*(\omega)}. \tag{6}$$

The numerical solution of Eq. (6) using Eqs. (2) and (3) yields the spectrum of the complex refractive index $n^*(\omega)$. This approach is free from the problems of nonideal reference surface and the φ_0 but requires precise mechanics, which guarantees that the rotation of the emitter and the detector does not change the optical path of THz radiation for more than a few microns.

IV. OUTLOOK

A number of further improvements can enhance the performance of the spectrometer and make it even more flexible. The upper frequency limit is given by the detector antenna. State-of-the-art THz antennas are able to detect frequencies as high as 5 THz.[17] By replacement of free-space optics by a fiber-optic system similar to that offered by Picometrix, Inc. a spectrometer requiring no readjustments at all can be created. To enable low-temperature measurements, a continous-flow cryostat or bath cryostat rather than a close-cycled one should be chosen since high amplitude vibrations of the latter make the precise positioning of a sample difficult.

ACKNOWLEDGMENTS

The authors are grateful to Petr Kužel of the Academy of Sciences of the Czech Republic for fruitful discussions. M. K. acknowledges support by the Graduiertenkolleg Physik Nonostrukturierter Festkörper of the Deutsche Forschungsgemeinschaft.

[1] M. C. Nuss and J. Orenstein, in *Millimeter an Submillimeter Wave Spectroscopy in Solids*, edited by G. Grüner, Topics in Applied Physics, Vol. 74 (Springer, Berlin, 1998), pp. 7–109.
[2] T.-I. Jeon and D. Grischkowsky, Appl. Phys. Lett. **72**, 3032 (1998).
[3] S. D. Brorson, R. Buhleier, I. E. Trofimov, J. O. White, Ch. Ludwig, F. F. Balakirev, H.-U. Habermeier, and J. Kuhl, J. Opt. Soc. Am. B **13**, 1979 (1996).
[4] I. Wilke, M. Khazan, C. T. Rieck, P. Kužel, T. Kaiser, C. Jaekel, and H. Kurz, J. Appl. Phys. **87**, 2984 (2000).
[5] D. M. Mittleman, R. H. Jakobsen, R. Neelamani, R. G. Baraniuk, and M. C. Nuss, Appl. Phys. B: Lasers Opt. **67**, 379 (1998).
[6] R. A. Cheville and D. Grischkowsky, J. Opt. Soc. Am. B **16**, 317 (1999).
[7] D. M. Mittleman, M. Gupta, R. Neelamani, R. G. Baraniuk, J. V. Rudd, and M. Koch, Appl. Phys. B: Lasers Opt. **68**, 1085 (1999).
[8] D. M. Mittleman, S. Hunsche, L. Boibin, and M. C. Nuss, Opt. Lett. **22**, 904 (1997).
[9] S. C. Howells and L. A. Schlie, Appl. Phys. Lett. **69**, 550 (1996).
[10] T.-I. Jeon and D. Grischkowsky, Appl. Phys. Lett. **72**, 3032 (1998).
[11] S. Spielman, B. Parks, J. Orenstein, D. T. Nemeth, F. Ludwig, J. Clarke, P. Merchant, and D. J. Lew, Phys. Rev. Lett. **73**, 1537 (1994).
[12] M. Khazan, I. Wilke, and C. Stevens, IEEE Trans. Appl. Supercond. **11**, 3537 (2001).
[13] C. W. Siders, J. L. W. Siders, A. J. Taylor, S.-G. Park, M. R. Melloch, and A. M. Weiner, Opt. Lett. **24**, 241 (1999).
[14] P. P. Woskov, D. R. Cohn, S. C. Han, A. Gatesman, R. H. Giles, and J. Waldman, Rev. Sci. Instrum. **65**, 438 (1994).
[15] *Handbook of Optical Constants of Solids*, edited by E. D. Palik (Academic, New York, 1985).
[16] M. Born and E. Wolf, *Principles of Optics*, 7th ed. (Cambridge University Press, Cambridge, 1999).
[17] D. Grischkowsky (private communication).

Downloaded 16 Jan 2002 to 128.113.8.139. Redistribution subject to AIP license or copyright, see http://ojps.aip.org/rsio/rsicr.jsp